

Surface-enhanced Raman scattering microchip fabricated by femtosecond laser

Cheng-Hsiang Lin,^{1,2} Lan Jiang,³ Hai Xiao,⁴ Shean-Jen Chen,¹ and Hai-Lung Tsai^{2,*}

¹Department of Engineering Science, National Cheng Kung University, Tainan 70101, Taiwan

²Department of Mechanical and Aerospace Engineering, Missouri University of Science and Technology, Rolla, Missouri 65409, USA

³Department of Mechanical and Automation Engineering, 3rd School, Beijing Institute of Technology, 100081, China

⁴Department of Electrical and Computer Engineering, Missouri University of Science and Technology, Rolla, Missouri 65409, USA

*Corresponding author: tsai@mst.edu

Received June 4, 2010; revised July 31, 2010; accepted August 6, 2010;
posted August 12, 2010 (Doc. ID 129558); published August 25, 2010

We report a surface-enhanced Raman scattering (SERS) microchip that is capable of measuring SERS signals of liquid samples with high sensitivity. The microdevice is an integration of a silicon-based SERS substrate, a multi-mode optical fiber (MMF), and a microchannel embedded in the photosensitive glass fabricated by the femtosecond laser followed by thermal treatment, wet etching, and annealing. The performance of the SERS microchip is evaluated by measuring rhodamine 6G using a 632.8 nm He–Ne laser at 4.3 mW excitation power, which reveals that the detection limit is lower than 10^{-10} M at a 1 s short accumulation time. © 2010 Optical Society of America

OCIS codes: 240.6695, 230.3990, 140.7090.

Recently, a technique using a femtosecond (fs) laser to precisely fabricate micro-optical devices on glass materials for various applications has attracted much interest [1]. The technique provides the capability to develop a “lab-on-a-chip” in analytical chemistry and biomedical applications, resulting in low reagent consumption, fast analysis, and compactness of the system [2]. An optical-fiber-assisted Fabry–Perot interferometer embedded in a glass chip fabricated by an fs laser on photosensitive Foturan glass has also been reported [3]. Foturan glass has the features of optical transparency and resistance to corrosion. This material machined by an fs laser realizes top-down one-step fabrication of three-dimensional micro-optical structures without additional assembly [4,5]. It greatly simplifies chip fabrication and makes it easier to achieve a complex design. By combining the glass microchip and SERS functionality, the dynamic structure and quantitative information of molecules can be detected with high sensitivity [6]. In this work, we employed the fs laser direct-writing technique to fabricate an SERS microchip that includes an SERS substrate, an optical fiber, and a microchannel embedded in the Foturan glass, demonstrating the capability of high-sensitivity SERS measurement of liquid samples.

The laser direct-writing process on a glass chip with microchannels, as well as on the SERS-active substrate, was carried out with an fs laser micromachining system that consists of an amplified fs laser (Legend-F, Coherent), a five-axis motion stage (Aerotech) with a resolution of $1\ \mu\text{m}$, and an inline imaging system to monitor the machining process. The delivered pulse energy was adjusted by a combination of a half-wave plate and a linear polarizer for different experimental requirements. The attenuated laser beam was directed into a $10\times$ microscope objective lens ($\text{NA} = 0.3$, Olympus) and focused on the sample, which was translated by the motion stage during processing.

The glass microchip with microchannels includes three major parts: sample inlet and outlet ports, a microchannel with one opened segment facing the wall of the chip and two buried segments, each connected to the

sample inlet and outlet, and a fiber holder. The sample inlet and outlet ports are each $0.5\ \text{mm} \times 0.5\ \text{mm}$ square and $0.2\ \text{mm}$ deep. The square microchannel, $120\ \mu\text{m} \times 120\ \mu\text{m}$, is $3\ \text{mm}$ and $0.5\ \text{mm}$ long, respectively, for the opened and buried segments. The center line of the channel is at a distance of $160\ \mu\text{m}$ below the surface. The fiber holder has a $300\text{-}\mu\text{m}$ -long fiber clamp followed by a 5-mm -long open groove. These microcomponents, as well as the chip boundaries, were simultaneously fabricated in a photosensitive Foturan glass. Foturan glass is a lithium–potassium glass doped with a trace amount of silver and cerium oxides [7]. When exposed to tightly focused fs pulses, some silver ions form silver atoms by capturing electrons released from the cerium ions (Ce^{3+}). In a subsequent heat treatment, the silver atoms agglomerate to form clusters, and then the crystalline phase of lithium metasilicate grows around the silver clusters, which can be preferentially etched away in a dilute solution of hydrofluoric acid, leaving behind the microstructures in the glass. After the modification process, the subsequent thermal treatment, wet etching, and annealing were conducted [7]. In this study, a 10% hydrofluoric acid was used and the etching process took about 25 min. The average surface roughness of the fabricated microstructures can be less than $1\ \text{nm}$ after the annealing process [5]. The optical image of the fabricated microchip in the photosensitive Foturan glass before inserting the optical fiber is shown in Fig. 1.

In SERS substrate fabrication, the cleaned silicon wafer substrates were dipped into 2 ml diluted aqueous solutions of silver nitrate with a concentration of $0.1\ \text{M}$ contained in an open vessel. The fs laser pulses were focused onto the sample via a $10\times$ objective lens ($\text{NA} = 0.3$), and the samples were translated by the motion stage during the line-by-line machining process. The scanning speed, scanning pitch, and delivered pulse energy were set as $1\ \text{mm}/\text{min}$, $1\ \mu\text{m}$, and $27\ \text{nJ}$ ($0.3\ \text{J}/\text{cm}^2$), respectively, and an active area of $200\ \mu\text{m} \times 120\ \mu\text{m}$ was fabricated. After the machining process, the samples were rinsed in deionized water to clean up the excess silver nitrate solution. The morphology of the produced

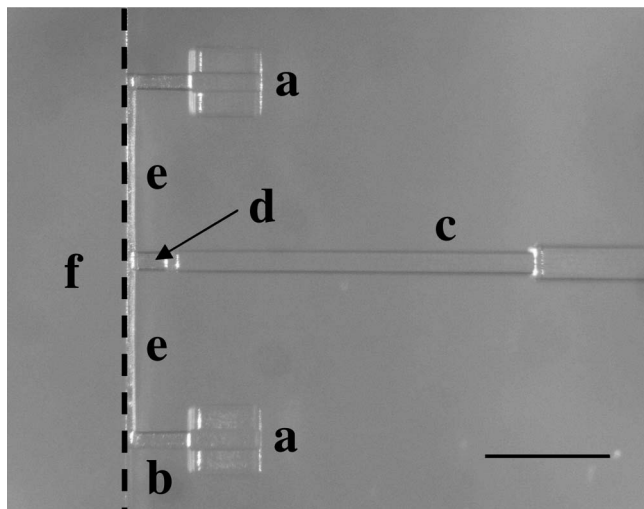


Fig. 1. Optical image of the glass microchip with a 1 mm scale bar. a, sample inlet/outlet ports opened to the top surface of the glass chip; b, embedded microchannels connecting a and e; c, an opened part of the fiber holder; d, an embedded fiber clamp; e, an embedded microchannel with an opened end along the side surface (dashed line) of the glass chip; and f, the SERS substrate is bound to the chip along the dashed line.

nanostructures was examined by scanning electron microscopy (SEM). The SERS substrate was bound to the glass chip using epoxy, as shown in Fig. 1(f).

Figures 2(a) and 2(b) show, respectively, the SEM image of the silicon wafer machined by an fs laser in deionized water and in 0.1 M aqueous solutions of silver nitrate at a scanning speed of 1 mm/min. In Fig. 2(a), the gratinglike periodic nanostructures have a sub-micrometer period, which agrees with previous studies [8–10]. Besides the gratinglike structures, no apparent particles are seen in Fig. 2(a). In contrast, in Fig. 2(b), after the sample was machined in the aqueous solutions of silver nitrate, nanoparticles attached to the machined surface are clearly seen. The silver nanoparticles were reduced from silver nitrate by fs laser pulses through multiphoton photon reduction [11]. The particle sizes range from tens to hundreds of nanometers, as evaluated from the enlarged SEM images. From the SEM image, the formation of the nanoparticles on the machined surface appears to be particle aggregations. The aggregation structures are proven to cause higher SERS enhancement factors due to the “hot spots” with strong electromagnetic field enhancement created in the nanogap

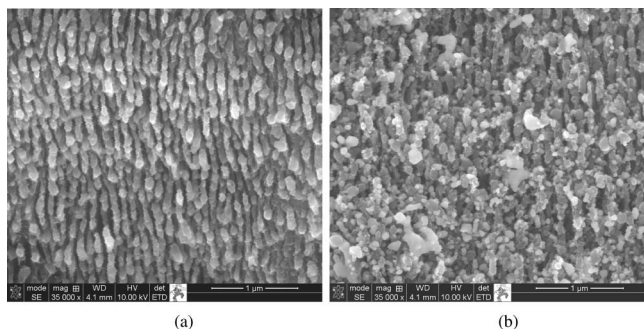


Fig. 2. Surface morphology of the silicon wafer substrate machined by fs laser pulses in (a) deionized water and (b) 0.1 M silver nitrate solutions at a scanning speed of 1 mm/min.

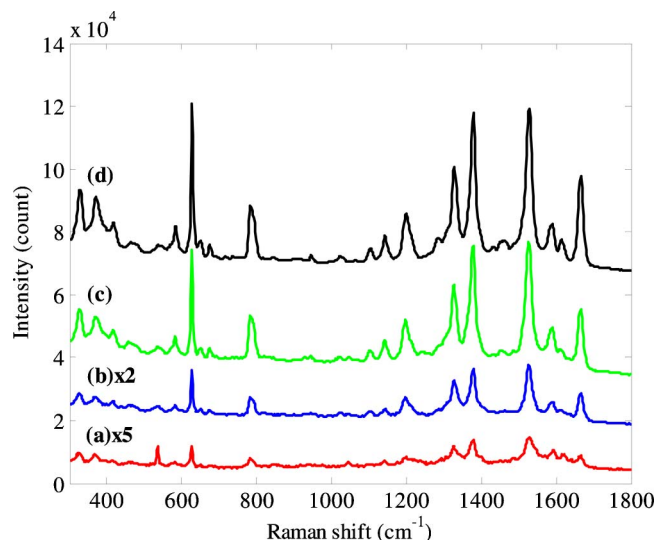


Fig. 3. (Color online) SERS spectra of R6G at concentrations of (a) 10^{-10} , (b) 10^{-9} , (c) 10^{-8} , and (d) 10^{-7} M.

between nanoparticles in the aggregation by localized plasmon coupling [12].

An MMF (Fiberguide 105/125Y) with a cleaved end surface was aligned as the end surface of the microchannel, and then the MMF was glued onto the fiber holder using epoxy. Finally, the fabricated SERS substrate was bound onto the glass microchip with the alignment of the active area right facing the end surface of the inserted MMF.

In SERS measurements, the aqueous solutions of rhodamine 6G (R6G) with concentrations of 10^{-3} to 10^{-10} M mixed with 10 mmol of sodium chloride were utilized to evaluate the performance of the SERS microchip. The Cl^- anions of sodium chloride were used to stabilize the adsorbent on the silver particles and to induce the electronic interaction between them [13]. All SERS measurements were conducted by means of a commercial Ramanscope (Jobin Yvon) integrated with an upright microscope using a He–Ne laser as a light source with a maximum excitation power of 17 mW. The employed laser excitation power and the signal accumulation time are adjustable with different sample concentrations to

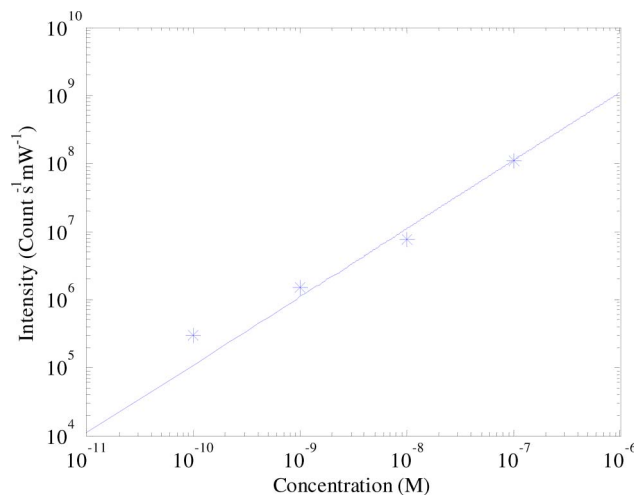


Fig. 4. (Color online) Normalized SERS intensities at different R6G concentrations.

achieve a better signal-to-noise ratio. The objective lens and grating used in this work were, respectively, $10\times$ ($\text{NA} = 0.25$) and 600 line/mm. The SERS microchip was connected to the Ramanscope through a MMF bound to the glass chip, and the excitation laser delivery and SERS signal collection were carried out remotely.

Figure 3 shows the SERS spectra of R6G at different concentrations, from 10^{-7} to 10^{-10} M. Note the accumulation time and laser power in the case of 10^{-7} M are, respectively, 0.5 s and 1.7 mW, but they were adjusted to 1 s and 4.3 mW for the cases of 10^{-8} , 10^{-9} , and 10^{-10} M. It is seen that the SERS signal of 10^{-10} M R6G is still detectable, which demonstrates the capability of high sensitivity SERS measurements of liquid samples at a 1 s short accumulation time. For comparison, the SERS signals at 614 cm^{-1} at different concentrations normalized by the excitation laser power and accumulation time are shown as Fig. 4. By linear fitting the data, the ideal detection limit at the conditions of a 1 s accumulation time and 1 mW of laser excitation power is about 10^{-17} M. This is achieved by extrapolating the data until the SERS intensity goes to zero. However, at this detection limit, the measurement may not be noise free. If a signal with an intensity of 100 counts is detectable, the detection limit is estimated to be about 10^{-15} M. The short accumulation time and low laser excitation power provide the capability of dynamic measurement and sample protection.

In conclusion, an on-chip SERS measuring microsystem that consists of a microchannel fabricated in Foturan glass and a silicon SERS substrate was demonstrated. The silicon SERS substrate fabricated by fs laser in silver nitrate solutions provides a high enhancement factor for high-sensitivity SERS measurements of R6G down to 10^{-10} M. The combination of the embedded microchip

and SERS substrate leads to the lab-on-a-chip's functionality, which can be further integrated with other functions to perform more complex measurements. The low excitation power promises the minimum sample heating and damaging.

This work was partially supported by the National Natural Science Foundation of China (NSFC) under grant 90923039 and the U.S. Department of Energy (DOE) under contract DE-FE0001127.

References

1. R. R. Gattass and E. Mazur, *Nat. Photon.* **2**, 219 (2008).
2. S. K. Hsiung, C. H. Lin, and G. B. Lee, *Electrophoresis* **26**, 1122 (2005).
3. C.-H. Lin, L. Jiang, H. Xiao, Y.-H. Chai, S.-J. Chen, and H.-L. Tsai, *Opt. Lett.* **34**, 2408 (2009).
4. C. H. Lin, L. Jiang, H. Xiao, Y. H. Chai, S. J. Chen, and H. L. Tsai, *Appl. Phys. A* **97**, 751 (2009).
5. Y. Cheng, K. Sugioka, and K. Midorikawa, *Opt. Lett.* **28**, 1144 (2003).
6. G. L. Liu and L. P. Lee, *Appl. Phys. Lett.* **87**, 074101 (2005).
7. T. Hongo, K. Sugioka, H. Niino, Y. Cheng, M. Masuda, I. Miyamoto, H. Takai, and K. Midorikawa, *J. Appl. Phys.* **97**, 063517 (2005).
8. J. E. Sipe, J. F. Young, J. S. Preston, and H. M. van Driel, *Phys. Rev. B* **27**, 1141 (1983).
9. J. F. Young, J. S. Preston, H. M. van Driel, and J. E. Sipe, *Phys. Rev. B* **27**, 1155 (1983).
10. J. F. Young, J. E. Sipe, and H. M. van Driel, *Phys. Rev. B* **30**, 2001 (1984).
11. H. Hada, Y. Yonezawa, A. Yoshida, and A. Kurakake, *J. Phys. Chem.* **80**, 2728 (1976).
12. I. W. Sztainbuch, *J. Chem. Phys.* **125**, 124707 (2006).
13. M. Futamata and Y. Maruyama, *Anal. Bioanal. Chem.* **388**, 89 (2007).